Available online at www.sciencedirect.com
ScienceDirect
Trans. Nonferrous Met. Soc. China 32(2022) 3610−3622
Transactions of Nonferrous Metals Society of China
www.tnmsc.cn

# Microstructure and mechanical properties evolution of 65Cu–35Zn brass tube during cyclic rotating−bending process

Zi-cheng ZHANG[1], Tsuyoshi FURUSHIMA[2], Ken-ichi MANABE[3]

1. School of Mechanical Engineering and Automation, Northeastern University, Shenyang 110819, China;
2. Department of Mechanical and Biofunctional Systems, Institute of Industrial Science, The University of Tokyo, Komaba 4-6-1, Meguro, Tokyo 153-8505, Japan;
3. Department of Mechanical Engineering, Tokyo Metropolitan University, 1-1 Minami-Osawa, Hachioji-shi, Tokyo 192-0397, Japan

Received 3 September 2021; accepted 14 February 2022

**Abstract:** The cyclic rotating−bending (CRB) processes under different deformation conditions were carried out to refine the microstructure and improve the mechanical properties of the 65Cu−35Zn brass tubes. The microstructure and the mechanical properties in the axial direction of the tubes after the CRB process were studied with the OM, EBSD and conventional tensile test. To obtain the accumulated effective plastic strain of the tube during the CRB process, the FEM simulation was also executed. The results show that the average grain size decreases with the increase of rotation time at RT, and with the decrease of bending angle at 200 °C. With the increase of accumulated effective plastic strain during the CRB process, the reduction rate of average grain size of the brass tube increases, the tensile strength of the brass tube increases in wave shape and the elongation increases first and then sharply decreases.

**Key words:** brass tube; cyclic rotating−bending process; severe plastic deformation; microstructure; mechanical properties

## 1 Introduction

The metallic tube has a wide application in the industry because of its high stiffness, lightweight, and hollow structure [1]. Generally, the metallic tubes are manufactured with the processes of hot-rolling, cold-rolling, cold-drawing, extruding and welding, etc. The metallic tubes produced with these conventional processes are often accompanied by the poor mechanical properties due to the microstructure consisting elongated and coarse grains or nonuniform grain distribution, which limited the applications of the metallic tubes. Although the metallic tubes with high strength and good ductility have a great application potential in industry, few efforts have been undertaken to produce the metallic tubes with fine grains and excellent mechanical properties.

In the material science research field, to refine the grains and improve the mechanical properties of the metallic materials, several kinds of severe plastic deformation (SPD) processes have been proposed in the recent years [2−5]. The SPD processes such as equal channel angular extrusion (ECAE) [6], repetitive side extrusion [7], rotary-die ECAP [8], parallel channel ECAP [9], accumulative roll-bonding (ARB) [10], and twist extrusion (TE) [11] have been successfully developed in the last several decades. Based on the traditional SPD process theory, some new kinds of SPD processes suitable for metallic tubes were also proposed, such as high-pressure tube twisting (HPTT) [12], incremental high pressure torsion (IHPT) [13],

**Corresponding author:** Zi-cheng ZHANG, Tel: +86-24-83674140, E-mail: zhangzicheng@me.neu.edu.cn
DOI: 10.1016/S1003-6326(22)66043-6

accumulative spin-bonding (ASB) [14], tubular channel angular pressing (TCAP) [15], parallel tubular channel angular pressing (PTCAP) [16], hydrostatic tube cyclic expansion extrusion (HTCEE) [17] and rotary extrusion (RE) [18]. However, the exiting SPD processes are mainly suitable for the grain refinement of the metal tubular materials with very short length. In addition, for most of the SPD processes mentioned above, the complex tools and large forming force are needed. The authors proposed a novel SPD technique of cyclic rotating−bending (CRB) process to refine the grain and improve the mechanical properties of the metallic tubes [19]. The accumulated cyclic compressive and tensile plastic strain in the deformation part of tube are used to refine the grains of the tubular materials. The tool of the CRB process is simple and the deformation force is low.

The pure copper and copper alloy have wide applications in electrical and automotive industries. To improve the mechanical properties of the pure copper, many efforts were implemented [20,21]. The exiting research report shows that for the copper alloy, the reducing grain size to near sub-micrometer or nanometer scale can effectively improve its mechanical properties such as strength, plasticity, hardness and fracture toughness [22]. There are several SPD processes used to refine the grain and improve the mechanical properties of the pure copper [17,23−27]. The constrained groove pressing (CGP) was used to refine the micro-structure of the copper alloy and the fine grains and improved mechanical properties of copper alloy were successfully obtained [28,29]. However, there are few researches related to the grain refinement and improvement of the mechanical properties of copper alloy tube by the SPD process.

In this study, the CRB process developed by the authors is utilized to refine the microstructure and improve the mechanical properties of the brass tube CuZn35 (ISO). The CRB processes with different deformation conditions were carried out to clarify the influence of the deformation parameters on the microstructure and mechanical properties evolution of brass tube. The microstructure of the brass tube processed by the CRB process was characterized with optical microscope (OM) and electron backscattered diffraction (EBSD). The mechanical properties such as strength and elongation were evaluated with conventional tensile test at RT. The FEM simulation was also implemented to obtain the accumulated effective plastic strain of the tube during the CRB process.

## 2 Experimental

The commercial extruded brass tube with a dimension of $d$10 mm (outside diameter) × 1 mm (wall thickness) × 200 mm (length) was employed in this study. The chemical composition and tensile properties such as ultimate tensile strength (UTS), yield strength (YS) and total elongation (EL) of the as-received brass tube are given in Table 1.

The schematic diagram of the CRB process proposed by the authors is shown in Fig. 1. The deformation part between the anti-friction bearings was heated with the high-frequency induction heating technique. When the temperature of the deformation part reached a certain value, the bending process began by moving anti-friction bearings. After the tube was bent, the driving-motor started to work to realize the rotation of the metal tube. The rotating bending process was kept for a given time with a certain rotation speed. Then, the anti-friction bearings returned to the original position to obtain the straight metal tube. The complex tools are not needed for the CRB process. It is suitable for process the tube or bar with large length and diameter.

Simultaneously, as the comparative references, the heat-treatment of the brass tubes were also executed with the temperatures and holding time same as the deformation temperatures and rotation time in the CRB processes. The bending angle of the tube is the key factor that influences the deformation intensity of the CRB process. The CRB processes with different bending angles were carried out to study the effect of the deformation

**Table 1** Chemical composition and mechanical properties of as-received brass tube

| Chemical composition/wt.% | | | | | Mechanical property | | |
|---|---|---|---|---|---|---|---|
| Cu | Zn | Pb | Fe | Total impurity | UTS/MPa | YS/MPa | EL/% |
| Bal. | 35.0 | ≤0.03 | ≤0.1 | ≤0.3 | 605 | 470 | 4.1 |

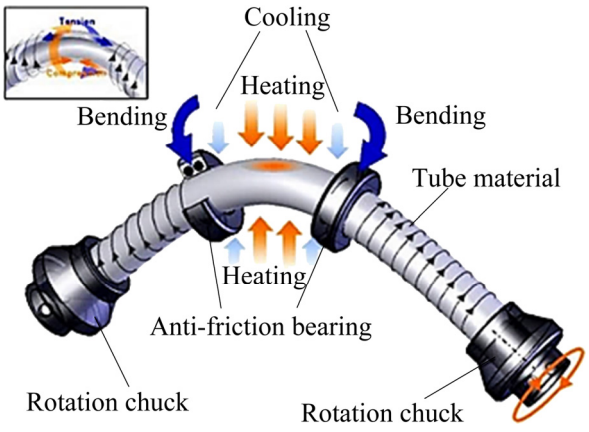


**Fig. 1** Schematic diagram of CRB process

intensity on the microstructure evolution of brass tube. The accumulated plastic strain has a strong influence on the grain refinement of materials in the SPD process. For the CRB process, the accumulated plastic strain is influenced by the deformation temperature, bending angle, rotation speed and rotation time. In the present study, the rotation speed of the CRB process was fixed to be 20 r/min. The bending angles of 171°, 174° and 177° were utilized with the deformation temperature of 200 °C and the rotation time of 5 min. The rotation time of 2, 5 and 8 min was adopted to investigate the influence of rotation time on the microstructure and mechanical properties evolution during the CRB processes carried out at room temperature (RT).

The apparatus for the CRB process used in this study is shown in Fig. 2. A high-frequency induction heating device with a maximum output power of 10 kW and a frequency range of 150−400 kHz (Type: EASYHEAT LI 8310) was employed to heat the deformation part of the tube. The ultra-compact digital radiation temperature sensor (KEYENCE FT−H40K) was conducted to measure the surface temperature of the deformation part of the tube. A water-cooling system was used to cool the tube parts under the anti-friction bearings to control the temperature distribution of the deformation part. A dial indicator was employed to measure the displacement of the bending bearings in the direction perpendicular to the axial direction of tube. The load cell was conducted to obtain the load on the bending bearings.

The specimens for microstructure investigation cut from the brass tubes along the axial direction were mounted with epoxy resin. After mechanical polishing, the specimens were etched in the solution of $FeCl_3$ and HCl (5 g $FeCl_3$ + 2 mL HCl + 100 mL $H_2O$) for 50 s. The OM (OLYMPUS BX51M) was used to observe the microstructure. The average grain sizes were measured with the linear interpret method. After mechanical polishing, the specimens were prepared with electrolytic polishing with a voltage of 3 V for 50 s in the mixed solution (300 mL deionized water + 200 mL $H_3PO_4$, + 50 mL $C_3H_8O$ + 2 g $CO(NH_2)_2$ + 4 g EDTA) for the EBSD analysis. The SEM (Zeiss Ultra Plus) equipped with EBSD was employed in this study. The tensile properties of the samples at RT were obtained with a universal test machine (SHIMADZU AG−50KN) with a fixed cross head speed of 2.5 mm/s. The specimens for the tensile test were prepared according to the standard of GB/T 228.1—2010 with an initial gauge length of 50 mm.

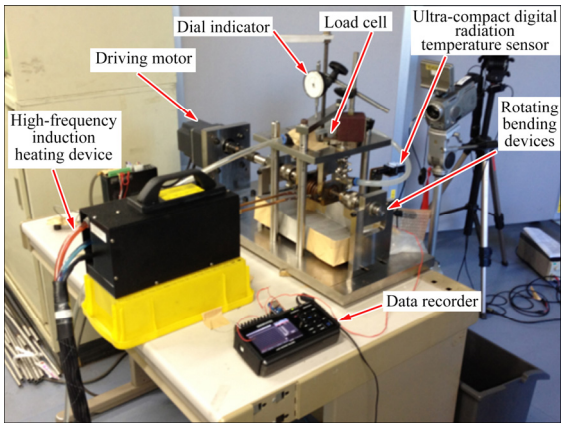


**Fig. 2** Apparatus of CRB process

## 3 FEM simulation

### 3.1 FEM model

The FEM simulation of the CRB process was carried out to obtain the accumulated effective plastic strain of the deformation part of the tube. The relationship between accumulated effective plastic strain and the average grain size reduction rate of the deformation part of the tube was determined with the FEM simulation results. A commercial code of ANSYS/LS-DYNA was employed in this study. The FEM model of the CRB process is presented in Fig. 3. In the FEM simulation, the chuck and bending bearings were assumed as the rigid bodies. The tube was assumed

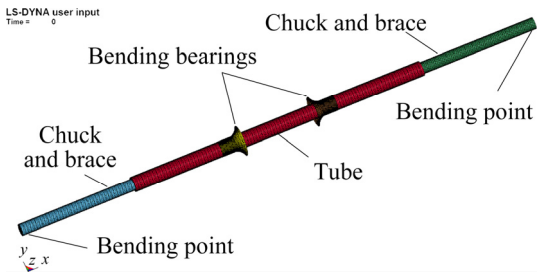


**Fig. 3** FEM model for CRB process

as the elastoplastic body. The friction coefficient between the bending bearings and tube was assumed to be 0.1 [30]. The initial temperatures of the bending bearings and chuck and brace to be set at RT. The temperature of the deformation part of the tube was set as the same as that in the experiments. The temperature of the rest parts of the tube were set as RT. The hexahedral solid element was used for the tube in the simulation. The element number of the tube was 12800. The parameters same as those in the experiment were used in the FEM simulation.

### 3.2 Verification of availability of FEM model

To verify the availability of FEM model, the load along the *Y*-axis direction acting on the bending bearing was examined in the experiment and FEM simulation. By comparing the load−time curves obtained in the experiment and FEM simulation, the availability of FEM model was confirmed. Figures 4(a, b) show the load−time curves obtained in the experiment and FEM simulation of CRB processes under the deformation

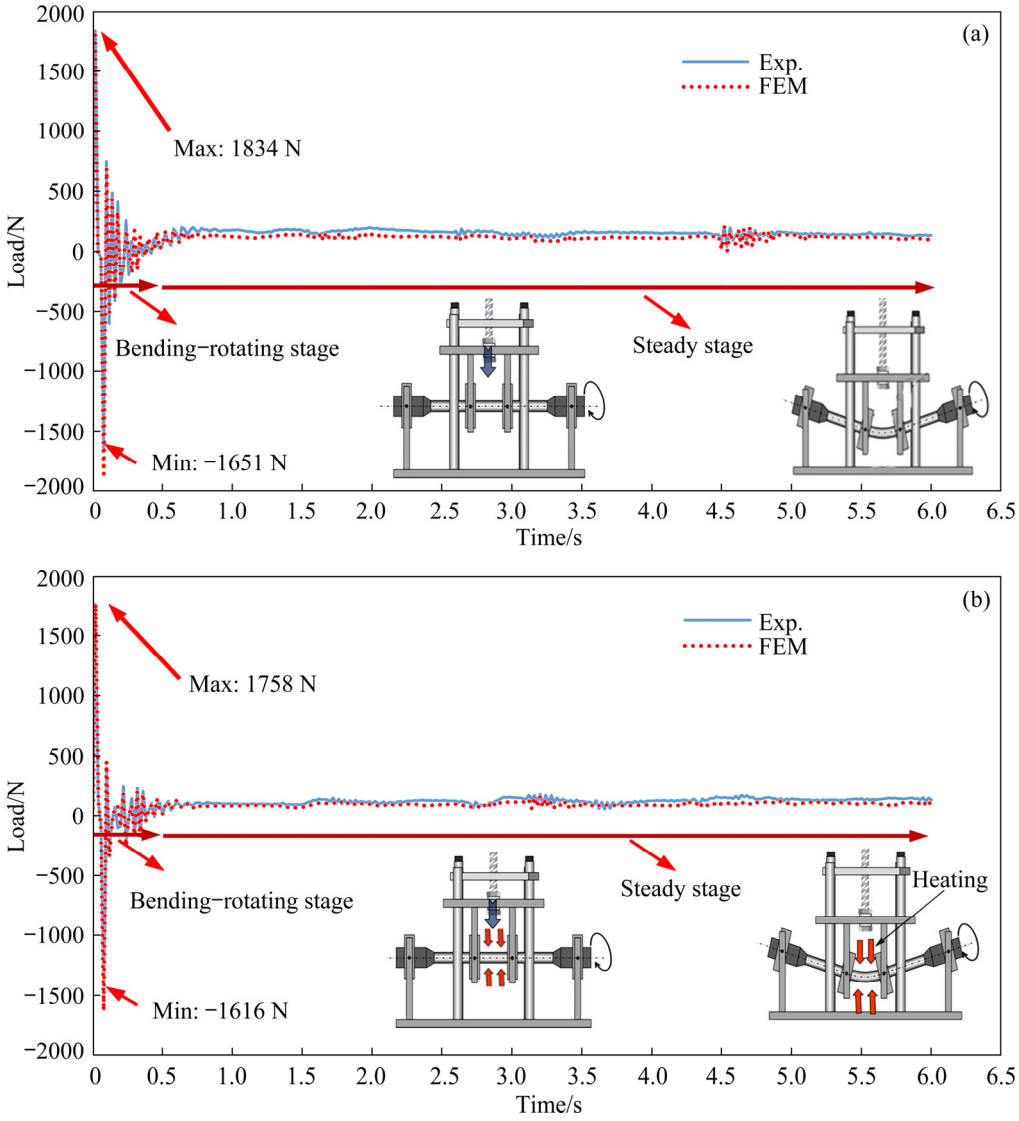


**Fig. 4** Load−time curves of bending bearings in CRB processes under different deformation conditions: (a) RT, 174°, 15 r/min, 6 s; (b) 200 °C, 174°, 20 r/min, 6 s

conditions (deformation temperature, bending angle, rotation speed and rotation time) of RT, 174°, 15 r/min, 6 s and 200 °C, 174°, 20 r/min, 6 s. It can be seen that the load−time curves obtained in the experiment and FEM simulation show a reasonable agreement. It also can be known that the FEM model is available both at RT and elevated temperature.

Form Fig. 4, it also can be known that the load on the bending bearings can be divided into two parts of bending−rotating stage and steady stage. It can be seen that the load increased rapidly in both positive and negative directions during the bending−rotating stage because the tube kept rotating during the bending process. The load is the bending force of the tube. The load became steady when the bending angle reached the predetermined value. In the steady stage, the tube rotated at the bending state. The load kept a certain value in the steady stage. The load value showed slightly fluctuating at the alternating time of the first turn and second turn. It also can be seen that with the same bending angle, the maximum load value was higher when the CRB process was carried out at RT than that when the CRB process was carried out at 200 °C.

## 4 Results and discussion

### 4.1 Microstructure

#### 4.1.1 Microstructure evolution with increase of rotation time at room temperature

When the other deformation parameters are fixed, the rotation time determines the accumulated effective plastic strain in the deformation part of the tube in the CRB process. In the current work, to study the effect of rotation time on the microstructure evolution at RT and elevated temperature, the CRB processes were performed with the rotation speed of 20 r/min, bending angle of 174°, rotation time of 2, 5 and 8 min at RT and deformation temperature of 200 °C, respectively.

Figure 5 shows the OM images of brass tubes processed by the CRB with the rotation time of 2, 5 and 8 min and the as-received tube. Figure 6 shows the average grain size of the as-received brass tube and the ones processed by the CRB. From Fig. 5, it can be seen that the $\alpha$-phase and $\beta$-phase grains are found in all the samples. The average grain sizes of the processed brass tubes are 83.95, 76.36 and 51.55 μm when the rotation time is 2, 5 and 8 min, respectively. The average grain size of the brass

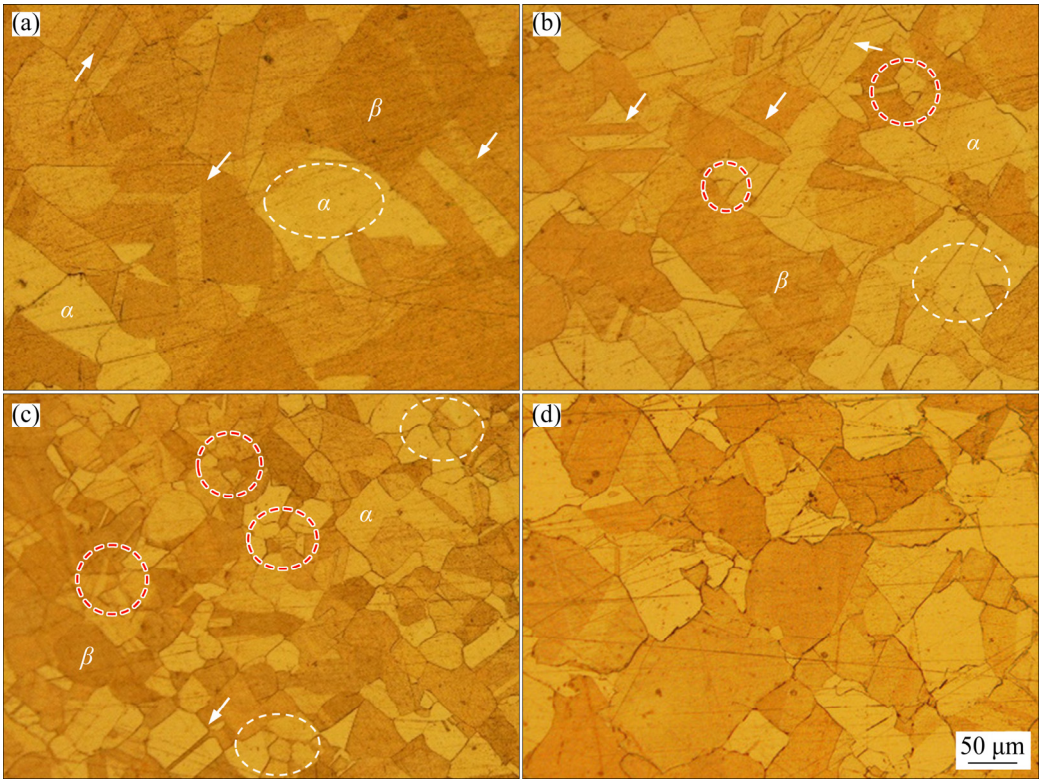


**Fig. 5** Metallographic observations of longitudinal section for brass tubes processed by CRB (RT, 174°, 20 r/min) with different rotation time: (a) 2 min; (b) 5 min; (c) 8 min; (d) As-received tube

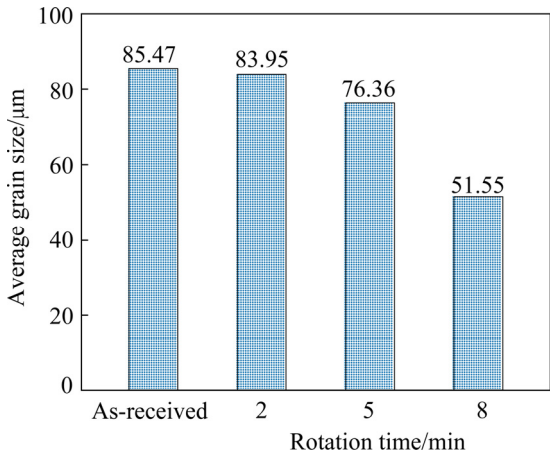


**Fig. 6** Effect of rotation time on average grain size of brass tube

tube processed by the CRB becomes smaller compared to that of the as-received tube. The average grain size decreases with the rotation time increasing from 2 to 8 min. From Fig. 5(a), it can be seen that the $\alpha$- and $\beta$-phase coarse grains can be found in the microstructure of the tube when the rotation time is 2 min. The big long twin structures (marked by the arrows) can also be seen in Fig. 5(a). With the rotation time increasing to 5 min, some coarse grains are refined. The large $\alpha$-phase grains are broken, as shown in Fig. 5(b) (marked by the white circle). The $\beta$-phase coarse grains are also partly refined. It can also be found that the area fraction of $\alpha$-phase grain is higher than that when the rotation time is 2 min. There are a lot of twins in the microstructure. Some new grains (marked by the red circles) appear in the microstructure, as shown in Fig. 5(b). When the rotation time is increased to 8 min, both $\alpha$- and $\beta$-phase grains are significantly refined (see Fig. 5(c)). The new grains (marked by the red circles) can be found in the microstructure of the sample. Only a few twins (marked by the white circle) can be found in the microstructure.

During the CRB process, the cyclic tensile and compressive severe plastic deformation not only leads to the fracture of the coarse grains but also the new grain nucleation along the twins and at the adjacent boundaries. The primarily responsible reasons for strain-induced grain size reduction are the dislocation activities for the copper alloy [31]. The dislocation movements, interactions and rearrangements lead to the formation of the substructure such as dislocation cells, dense dislocation walls, and tangles in the original coarse grains. The interactions between the substructures and the newly formed dislocations lead to the forming of the low angle boundaries and finally result in the division of the original coarse grains into smaller blocks. For the refinement of twins, it can be speculated as the lamellar structure formation and that is further subdivided into nanograins. When the rotation time is 5 min, the microtwins with high density are formed and converse the coarse grains into a lamellar structure, as shown in Fig. 5(b). It can also be speculated that with the increase of the accumulated plastic strain, the dislocation walls inside twin lamellae develop and the lamellar structure is further subdivided into equiaxed nanosized blocks. The preferentially orientated blocks become the randomly orientated nanograins. The nanograins grow into the small grains and finally an approximately homogeneous distribution of grains is achieved, as shown in Fig. 5(c).

4.1.2 Microstructure evolution with increase of rotation time at 200 °C

Figure 7 shows the EBSD orientation maps, distribution of high and low angle grain boundaries as well as misorientation of the samples processed by the CRB with the rotation time of 2, 5 and 8 min at 200 °C. Under the same deformation conditions, the average grain size of the tube processed by the CRB increases with the increase of the rotation time from 2 to 8 min, as shown in Figs. 7(a, b, c). When the deformation temperature is 200 °C, with the same bending angle and rotation speed, the rotation time shows a significant influence on the average size of the processed brass tube. The gains grow up with the increase of the deformation time at the deformation temperature of 200 °C. It can be deduced that at this temperature the grain grows up rapidly, and the effect of the plastic deformation on the grain refinement is smaller than the grain growth speed. Figure 7(d) shows the microstructure of the tube without deformation, which was only heat-treated at 200 °C for 8 min. Under the same temperature 1200 °C and time (8 min) conditions, the average grain size of the tube processed by the CRB (see Fig. 7(c)) is smaller than that of the only heat-treated tube (see Fig. 7(d)). This means that under the same temperature and time condition, the grains are refined by the CRB process.

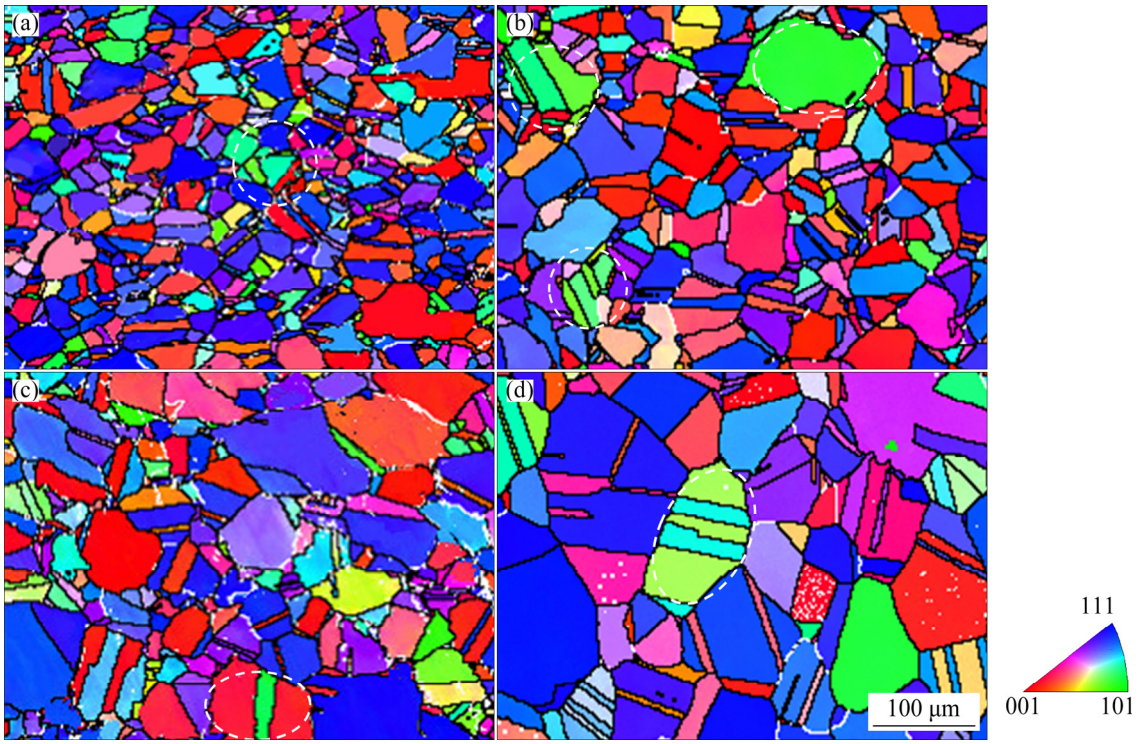


**Fig. 7** EBSD orientation maps and distribution of high and low angle grain boundaries misorientation of tubes processed by CRB processes under deformation conditions of 200 °C, 174°, 20 r/min ((a) 2 min, (b) 5 min, and (c) 8 min) and ones heat-treated at 200 °C for 8 min (d)

From Fig. 7, it also can be known that the orientation of the grains is also influenced by the deformation condition of the CRB process. The area fraction of the grains orientated in (or closest) (001)-direction increases with the rotation time increasing from 2 to 8 min. However, the area fraction of the grains orientated in (or closest) (111)-direction decreases with the increase of rotation time. The average size of the grains orientated in (or closest) (111)-direction increases with the increase of rotation time. The grains orientated in (or closest) (101)-direction mostly appear as twins in the microstructure.

Figure 8 shows the misorientation of the samples without deformation and the ones processed by the CRB with different rotation time under the deformation conditions of 200 °C, 174°, and 20 r/min. It can be seen that misorientation of all the samples mainly distributes in the range from 0° to 5° as well as from 55° to 65°. When the deformation time is 8 min, the relative frequency of the misorientation (RFM) distributing in the range from 55° to 65°of the sample processed by the CRB is about 35%, while that of the only heat-treated (200 °C for 8 min) sample is about 50%. For all the

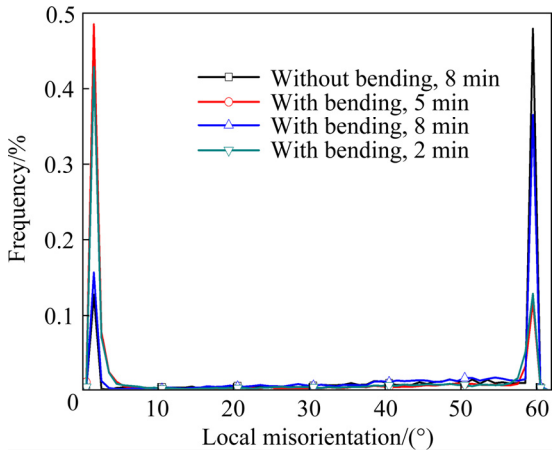


**Fig. 8** Misorientation of tubes without deformation and ones processed by CRB (200 °C, 174°, 20 r/min) with different rotation time

deformed samples, with the increase of the rotation time, the RFM distributing in the range from 55° to 65° shows a trend of decrease first and then a trend of increase. But the RFM distributing in the range from 55° to 65° of the deformed samples does not show much difference when the rotation time is 2 or 5 min. However, the RFM distributing in the range from 0° to 5° of the sample processed by the CRB with 5 min is about 50%, while that of the sample

processed by the CRB with 2 min is about 43%. When the rotation time is 8 min, the RFM distributing in the range from 0° to 5° is about 15%. For the heat-treated sample, the RFM distributing in the range from 0° to 5° is about 13%. From the misorientation distribution curves, it can be seen that the RFM distribution in the range from 0° to 5° presents an opposite tendency to that in the range from 55° to 65° when the rotation time is increased from 2 to 8 min.

Figure 9 shows the recrystallization diagram and distribution of high and low angle grain boundaries of the tubes processed by the CRB with different rotation time at of 200 °C. It can be seen that with the increase of the rotation time, the average grain size of the samples increases. The fraction of substructure increases first and then decreases with the increase of rotation time (see Fig. 9(d)). The area fraction of the recrystallized grain does not change much when the rotation time is increased from 2 to 5 min, but it increases sharply when the rotation time is increased from 5 to 8 min. However, the area fraction of the deformed grains decreases with the increase of the rotation time. Generally, at the same deformation rate, the accumulated plastic strain increases with the increase of the deformation time. However, in this study, for the samples processed by the CRB, the area fraction of the deformed grains decreases with the increase of the rotation time. It can be known that the recrystallization occurs in the deformed grains, which can also be confirmed by the area fraction of the recrystallization grains (see Fig. 9(d)).

4.1.3 Microstructure evolution with decrease of bending angle

Figure 10 shows the microstructure of the samples processed by the CRB with different bending angles and that of the heat-treated sample. Figure 11 shows the average grain size of the heat-treated sample and the samples processed by the CRB processes with different bending angles. The average grain size of the heat-treated sample is about 86.8 μm. With the bending angle decreasing from 177° to 171°, the average grain size decreases from 69.05 to 32.17 μm. It can be seen that the grains are refined by the CRB process compared with that of the heat-treated sample. The bending angle has the significant influence on the refinement of the grains during the CRB process (see Figs. 10(b, c, d)).

The $\alpha$-phase and $\beta$-phase can be found in the

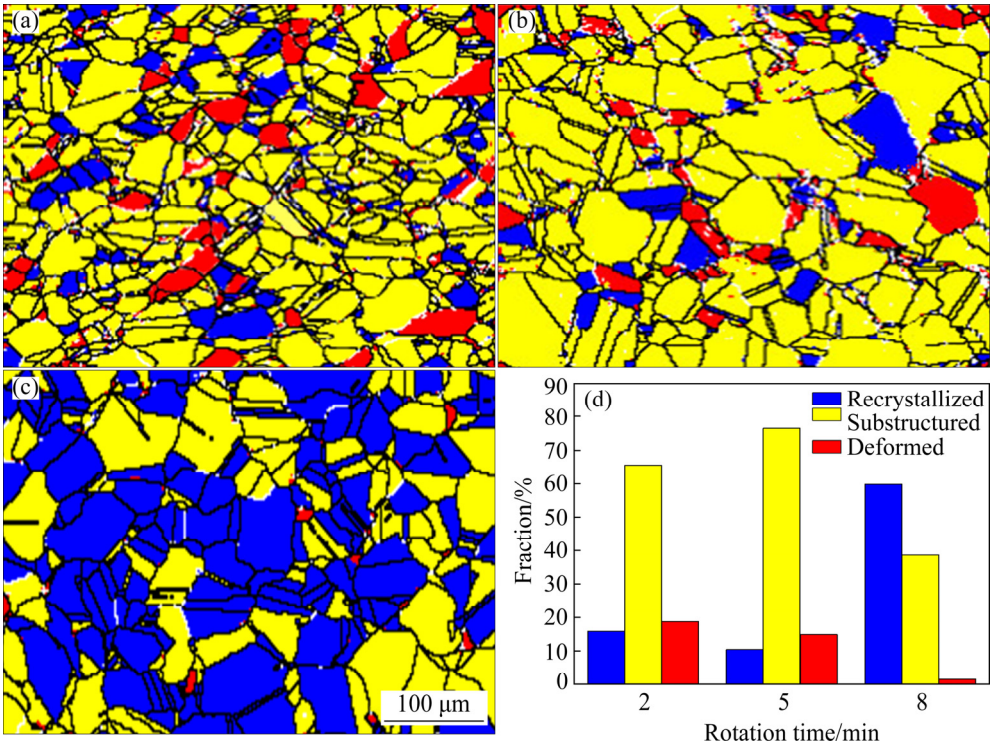


**Fig. 9** Recrystallization diagram and distribution of high and low angle grain boundaries of samples processed by CRB (200 °C, 174°, 20 r/min) with different deformation time ((a) 2 min, (b) 5 min, and (c) 8 min) and relationship between rotation time and fraction of different structures (d)

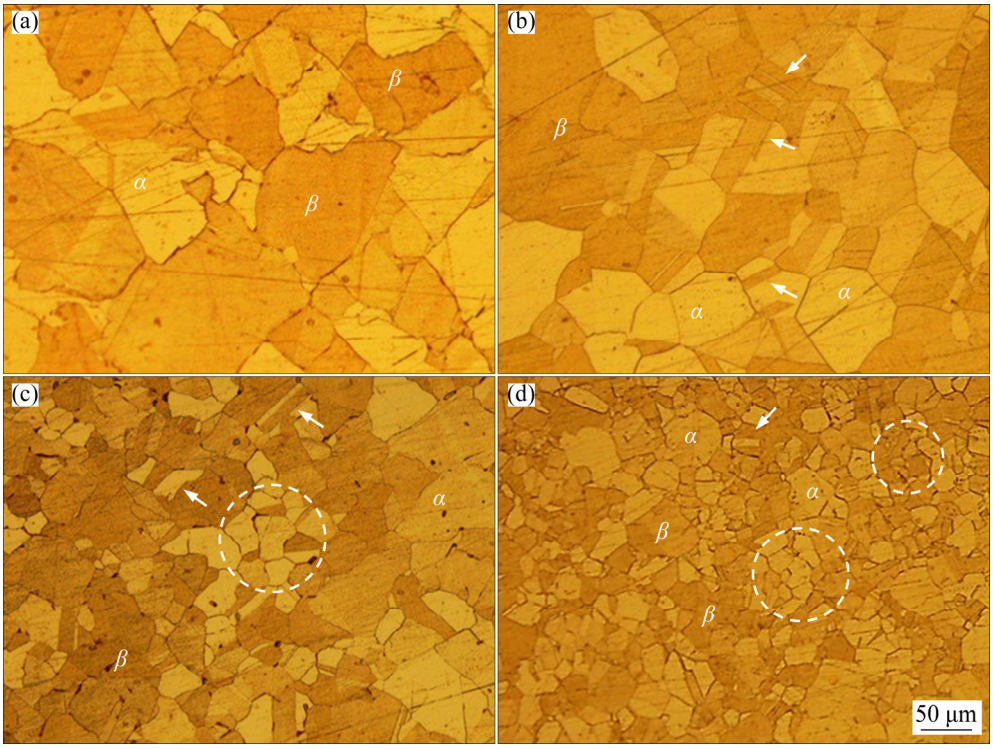


**Fig. 10** Effect of bending angles on microstructure of brass tubes heat-treated at 200 °C for 5 min (a) and processed by CRB (200 °C, 5 min, 20 r/min) with different bending angles ((b) 177°, (c) 174°, and (d) 171°)

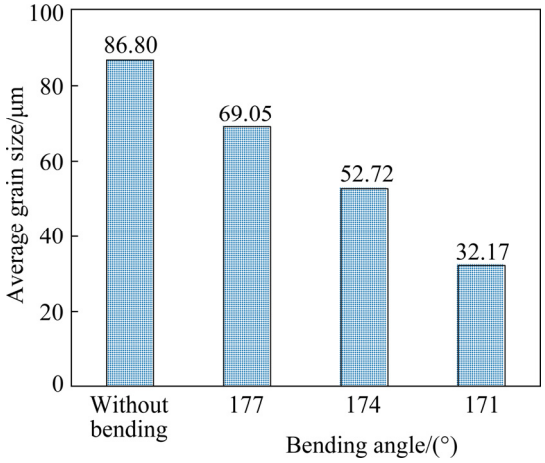


**Fig. 11** Average grain size of tubes without bending and processed by CRB (200 °C, 5 min, 20 r/min) with different bending angles

microstructure of all the samples. The $\alpha$- and $\beta$-phase coarse grains uniformly distribute in the microstructure of the heat-treated sample. The $\alpha$- and $\beta$-phase grains are smaller and the twins (indicated by the arrows in Fig. 10(b)) can be found in the microstructure of the sample processed by the CRB with bending angle of 177°. When the bending angle of 174° is adopted in the CRB process, the grains of sample processed by the CRB become smaller and the area fraction of the twins in the microstructure becomes lower. A few of $\alpha$- and $\beta$-phase coarse grains can be found in the microstructure. The $\beta$-phase coarse grains are refined by the severe plastic deformation during the CRB process (indicated by the circle in Fig. 10(c)). However, when the bending angle of 171° is utilized in the CRB process, the grains of the sample are heavily refined in the CRB process. The twin area fraction becomes lower further. Few $\alpha$- and $\beta$-phase coarse grains are found in the microstructure (see Fig. 10(d)).

4.1.4 Relationship between accumulated effective plastic strain and reduction rate of average grain size

Figure 12 shows the reduction rate of average grain size of 65Cu−35Zn brass tube with the accumulated effective plastic strain obtained with FEM simulation. It can be known that the reduction rate of average grain size increases with the increase of the accumulated effective plastic strain during the CRB process under the conditions of 200 °C, 174°, and 20 r/min with different rotation time. From the curve, it can be known that the accumulated effective plastic strain has a strong influence on the refinement of the grain of the sample during the CRB process. During the CRB

process, the accumulated heavy effective plastic strain leads to the boundary migration and bulging, resulting in the boundary fluctuations in shape. The boundary fluctuations develop into the serrations that are the actual nucleation sites [32,33]. The fragmentation of coarse grain and new grain forming caused by the severe plastic deformation finally lead to the refinement of the microstructure. Moreover, the heavy plastic strain also leads to the dislocation migration and generation because of the incompatibilities among grains.

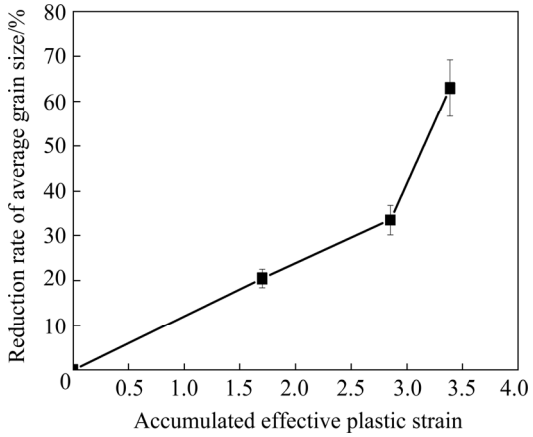


**Fig. 12** Reduction rate of average grain size of 65Cu−35Zn brass tube with accumulated effective plastic strain (200 °C, 174°, 20 r/min)

## 4.2 Mechanical properties

### 4.2.1 Mechanical properties evolution with increase of rotation time

Figure 13 shows the effect of the rotation time on the mechanical properties of the tubes processed by CRB. The strength decreases and the elongation increases of the tubes processed by CRB compared to those of the as-received tube. When the rotation time is increased from 2 to 8 min, the elongation of the tubes processed by CRB increases first and then decreases. The strength of the tube processed by CRB decreases first and then increases with the rotation time increasing from 2 to 8 min. The coarse grains and the residual work hardening in the deformation process of the tube lead to the high strength and the poor elongation of the as-received tube. The severe plastic deformation in the CRB process results in the large amount of lattice distortion and the substructures in the tube, which provides nucleation conditions for the recrystallization. With the increase of the rotation time, more grains nucleate and grow up. The refined microstructure leads to the improvement of the ductility of the tube.

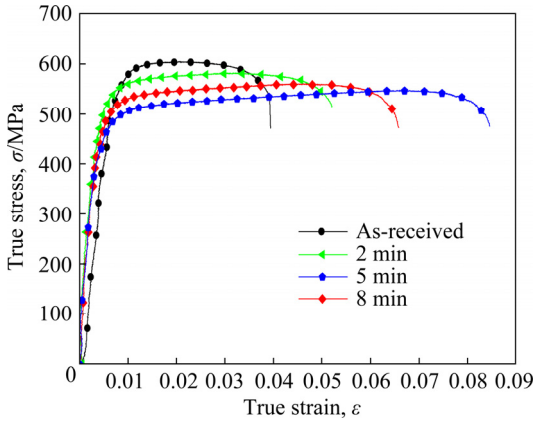


**Fig. 13** True stress versus true strain curves of as-received tube and ones processed by CRB (RT, 174°, 20 r/min) with different rotation time

### 4.2.2 Mechanical properties evolution with decrease of bending angle

Figure 14 shows the true stress versus true strain curves of the heat-treated (200 °C, 5 min) brass tube and the ones processed by CRB with the bending angles of 171°, 174° and 177°. It can be seen that the heat-treated tube (without bending) shows poor tensile strength and elongation compared to the tubes processed by CRB. When the bending angle of 171° is adopted in the CRB process, the processed tube shows the best tensile strength and ductility. The tube processed by CRB with the bending angle of 177° shows good ductility but poor tensile strength. The elongation of the processed tubes by the CRB process shows a trend of decreasing first and then increasing with the bending angle is increased from 171° to 177°. However, the tensile strength of the tubes processed by CRB decreases with the increase of the bending angle. For the heat-treated tube, the coarse grains result in the poor ductility (see Fig. 10(a)). The grain refinement of the tubes processed by CRB with different bending angles leads to the improvement of their ductility. When the bending angle is small, the plastic deformation is much severer and improves the grain refinement efficiency. In the meantime, the work hardening produced in the CRB process leads to the increase of the tensile strength. Therefore, in this study, both of the strength and the elongation of the tubes processed by CRB with different bending angles are improved.

4.2.3 Relationship between accumulated effective plastic strain and mechanical properties

Figure 15 shows the relationship between tensile strength as well as elongation and accumulated effective plastic strain of the tubes processed by CRB. It can be seen that the tensile strength of the tube increases in wave shape with the increase of the accumulated effective plastic strain increasing from zero to 3.5. The elongation of the tube increases with the increase of the accumulated effective plastic strain. However, it shows a sharp decrease when the accumulated effective plastic strain is increased from 2.75 to 3.5. The severe plastic strain in the CRB process causes recrystallization and work hardening at the same time. The work hardening improves the tensile strength of the tube. The recrystallization results in the refinement of the grains, which finally leads to the improvement of the ductility of the tube. However, when the accumulated effective plastic strain reaches a certain value, the work hardening far outweighs softening caused by the recrystallization, and this is the reason for the tensile strength of the tube increasing and the elongation of the tube decreasing sharply.

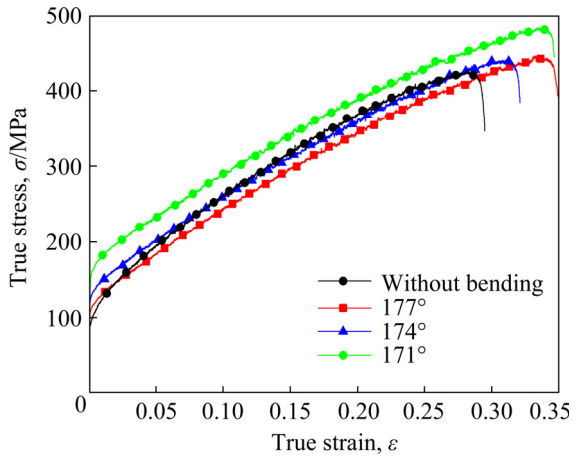


**Fig. 14** True stress vs true strain curves of heat-treated brass tube and ones processed by CRB (200 °C, 20 r/min, 5 min) with different bending angles

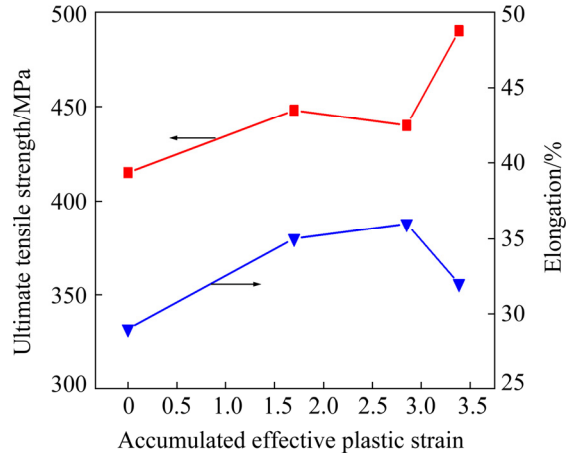


**Fig. 15** Relationship between tensile strength as well as elongation and accumulated effective plastic strain of tubes processed by CRB (200 °C, 174°, 20 r/min)

## 5 Conclusions

(1) The average grain size decreases with the increase of the rotation time at RT, and with the decrease of the bending angle at the deformation temperature of 200 °C.

(2) With the rotation time increasing from 2 to 8 min, the tensile strength of the tubes processed by CRB under the deformation condition of RT, 174°, 20 r/min decreases first and then increases, and the elongation of the tube increases first and then decreases. The tensile strength of the tubes decreases and the elongation decreases first and then increases with the bending angle increasing from 171° to 177° of CRB-processed tube under the deformation condition of 200 °C, 20 r/min, 5 min.

(3) The reduction rate of average grain size increases with the increase of the accumulated effective plastic strain during the CRB process under the deformation conditions of 200 °C, 174°, 20 r/min. The tensile strength of the tube increases in wave shape with the increase of the accumulated effective plastic strain increasing from zero to 3.5 and the elongation of the tube increases with the increase of the accumulated effective plastic strain; however, it shows a sharp decrease when the accumulated effective plastic strain is increased from 2.75 to 3.5.

## Acknowledgments

The authors are grateful for the financial supports from the National Natural Science Foundation of China (No. 51304046), and the Grant-in-Aid for Young Scientists (B) of Japan Society for the Promotion of Science of Japan (No. 25870594)

## References

[1] BAROUTAJI A, SAJJIA M, OLABI A G. Metallic thin-walled tubes for crashworthiness applications: A reference guide [M]//Reference Module in Materials Science and

Materials Engineering. Elsevier, 2017.

[2] AZUSHIMA A, KOPP R, KORHONEN A, YANG D Y, MICARI F, LAHOTI G D, GROCHE P, YANAGIMOTO J, TSUJI N, ROSOCHOWSKI A, YANAGIDA A. Severe plastic deformation (SPD) processes for metals [J]. CIRP Annals-Manufacturing Technology, 2008, 57(2): 716−735.

[3] KULAGIN R, BEYGELZIMER Y, BACHMAIER A, PIPPAN R, ESTRIN Y. Benefits of pattern formation by severe plastic deformation [J]. Applied Materials Today, 2019, 15: 236−241.

[4] FARAJI G, KIM H S, KASHI H T. Severe plastic deformation [M]. Elsevier, 2018.

[5] SIAHSARANI A, FARAJI G. Processing and characterization of AZ91 magnesium alloys via a novel severe plastic deformation method: Hydrostatic cyclic extrusion compression (HCEC) [J]. Transactions of Nonferrous Metals Society of China, 2021, 31(5): 1303−1321.

[6] SEGAL V M. Equal channel angular extrusion: From macromechanics to structure formation [J]. Materials Science and Engineering A, 1999, 271(1/2): 322−333.

[7] AZUSHIMA A, AOKI K. Mechanical properties of ultrafine grained steel produced by repetitive cold side extrusion [J]. CIRP Annals−Manufacturing Technology, 2002, 51(1): 227−230.

[8] NISHIDA Y, ARIMA H, KIM J C, ANDO T. Rotary-die equal-channel angular pressing of an Al−7mass.%Si−0.35mass.%Mg alloy [J]. Scripta Materialia, 2001, 45: 261−266.

[9] DJAVANROODI F, EBRAHIMI M. Effect of die parameters and material properties in ECAP with parallel channels [J]. Materials Science and Engineering A, 2010, 527: 7593−7599.

[10] SAITO Y, UTSUNOMIYA H, TSUJI N, SAKAI T. Novel ultra-high straining process for bulk materials-development of the accumulative roll-bonding (ARB) process [J]. Acta Materialia, 1999, 47(2): 579−583.

[11] BEYGELZIMER Y, RESHETOV A, SYNKOV S, PROKOF'EVA O, KULAGIN R. Kinematics of metal flow during twist extrusion investigated with a new experimental method [J]. Journal of Materials Processing Technology, 2009, 209(7): 3650−3656.

[12] TÓTH L S, ARZAGHI M, FUNDENBERGER J J, BEAUSIR B, BOUAZIZ O, ARRUFFAT-MASSION R. Severe plastic deformation of metals by high-pressure tube twisting [J]. Scripta Materialia, 2009, 60: 175−177.

[13] HOHENWARTER A. Incremental high pressure torsion as a novel severe plastic deformation process: Processing features and application to copper [J]. Materials Science and Engineering A, 2015, 626: 80−85.

[14] MOHEBBI M S, AKBARZADEH A. Accumulative spin-bonding (ASB) as a novel SPD process for fabrication of nanostructured tubes [J]. Materials Science and Engineering A, 2010, 528: 180−188.

[15] FARAJI G, MASHHADI M M, KIM H S. Tubular channel angular pressing (TCAP) as a novel severe plastic deformation method for cylindrical tubes [J]. Materials Letters, 2011, 65: 3009−3012.

[16] FARAJI G, BABAEI A, MASHHADI M M, ABRINIA K. Parallel tubular channel angular pressing (PTCAP) as a new severe plastic deformation method for cylindrical tubes [J]. Materials Letters, 2012, 77: 82−85.

[17] MOTALLEBI SAVARABADI M, FARAJI G, ZALNEZHAD E. Hydrostatic tube cyclic expansion extrusion (HTCEE) as a new severe plastic deformation method for producing long nanostructured tubes [J]. Journal of Alloys and Compounds, 2019, 785: 163−168.

[18] ABDOLVAND H, SOHRABI H, FARAJI G, YUSOF F. A novel combined severe plastic deformation method for producing thin-walled ultrafine grained cylindrical tubes [J]. Materials Letters, 2015, 143: 167−171.

[19] ZHANG Zi-cheng, SHAO Shuai, MANABE K I, KONG Xiang-wei, LI Yan-mei. Evolution of microstructure and mechanical properties of Al 6061 alloy tube in cyclic rotating bending process [J]. Materials Science and Engineering A, 2016, 676: 80−87.

[20] SEIFOLLAHZADEH P, ALIZADEH M, ABBASI M R. Strength prediction of multi-layered copper-based composites fabricated by accumulative roll bonding [J]. Transactions of Nonferrous Metals Society of China, 2021, 31(6): 1729−1739.

[21] LI Hai-hong, LIU Xiao, LI Yang, ZHANG Shi-hong, CHEN Yan, WANG Song-wei, LIU Jin-song, WU Jin-hu. Effects of rare earth Ce addition on microstructure and mechanical properties of impure copper containing Pb [J]. Transactions of Nonferrous Metals Society of China, 2020, 30(6): 1574−1581.

[22] VALIEV R Z, ISLAMGALIEV R K, ALEXANDROV I V. Bulk nanostructured materials from severe plastic deformation [J]. Progress in Materials Science, 2000, 45(2): 103−189.

[23] WEI Wei, CHEN Guang, WANG Jing-tao, CHEN Guo-liang. Microstructure and tensile properties of ultrafine grained copper processed by equal-channel angular pressing [J]. Rare Metals, 2006, 25(6): 697−703.

[24] QI Yuan-shen, KOSINOVA A, KILMAMETOV A R, STRAUMAL B B, RABKIN E. Stabilization of ultrafine-grained microstructure in high-purity copper by gas-filled pores produced by severe plastic deformation [J]. Scripta Materialia, 2020, 178: 29−33.

[25] EDALATI K, CUBERO-SESIN J M, ALHAMIDI A, MOHAMED I F, HORITA Z. Influence of severe plastic deformation at cryogenic temperature on grain refinement and softening of pure metals: Investigation using high-pressure torsion [J]. Materials Science and Engineering A, 2014, 613: 103−110.

[26] BABAEI A, MASHHADI M M. Tubular pure copper grain refining by tube cyclic extrusion-compression (TCEC) as a severe plastic deformation technique [J]. Progress in Natural Science: Materials International, 2014, 24(6): 623−630.

[27] WANG Cheng-peng, LI Fu-guo, LI Qing-hua, WANG Lei. Numerical and experimental studies of pure copper processed by a new severe plastic deformation method [J]. Materials Science and Engineering A, 2012, 548: 19−26.

[28] PENG Kai-ping, SU Li-feng, SHAW L L, QIAN K W. Grain refinement and crack prevention in constrained groove pressing of two-phase Cu−Zn alloys [J]. Scripta Materialia, 2007, 56: 987−990.

[29] PENG Kai-ping, ZHANG Ying, SHAW L L, QIAN K W. Microstructure dependence of a Cu−38Zn alloy on processing conditions of constrained groove pressing [J]. Acta Materialia, 2009, 57(18): 5543−5553.
[30] MIRZAI M A, MANABE K I, MABUCHI T. Deformation characteristics of microtubes in flaring test [J]. Journal of Materials Processing Technology, 2008, 201(1): 214−219.
[31] VERLEYSEN P, LANJEWAR H. Dynamic high pressure torsion: A novel technique for dynamic severe plastic deformation [J]. Journal of Materials Processing Technology, 2020, 276: 116393.
[32] BELYAKOV A, MIURA H, TAKU S. Dynamic recrystallization under warm deformation of polycrystalline copper [J]. ISIJ International, 1998, 38(6): 595−601.
[33] SAKAI T, BELYAKOV A, KAIBYSHEV R, MIURA H, JONAS J J. Dynamic and post-dynamic recrystallization under hot, cold and severe plastic deformation conditions [J]. Progress in Materials Science, 2014, 60: 130−207.

# 循环旋转弯曲变形中 65Cu–35Zn 黄铜管显微组织和力学性能的演变

张自成[1]，Tsuyoshi FURUSHIMA[2], Ken-ichi MANABE[3]

1. 东北大学 机械工程与自动化学院，沈阳 110819；
2. Department of Mechanical and Biofunctional Systems, Institute of Industrial Science, The University of Tokyo, Komaba 4-6-1, Meguro, Tokyo 153-8505, Japan;
3. Department of Mechanical Engineering, Tokyo Metropolitan University, 1-1 Minami-Osawa, Hachioji-shi, Tokyo 192-0397, Japan

**摘　要：**为了细化 65Cu−35Zn 黄铜管的晶粒尺寸，并改善其力学性能，进行不同变形条件下的循环旋转弯曲(CRB)实验。利用光学显微镜、EBSD 和常温拉伸实验，对变形后管材的显微组织和轴向力学性能进行研究。为了获得变形过程中黄铜管的累计有效塑性应变，对黄铜管不同变形条件下的 CRB 进行有限元模拟。结果表明，常温变形条件下，黄铜管的平均晶粒尺寸随旋转时间的增加而减小；在 200 ℃变形条件下，其平均晶粒尺寸随弯曲角度的减小而减小。随着累计有效塑性应变的增加，变形后黄铜管平均晶粒尺寸减小率呈现增大趋势，其抗拉强度呈现波状增加，而伸长率呈现先增加后迅速减小的趋势。

**关键词：**黄铜管；循环旋转弯曲工艺；剧烈塑性变形；显微组织；力学性能

**(Edited by Bing YANG)**